Anatomical and functional abnormalities on MRI in kabuki syndrome

Jennifer Boisgontier, Jean Marc Tacchella, Hervé Lemaitre, Natacha Lehman, Ana Saitovitch, Vincent Gatinois, Guilaine Boursier, Elodie Sanchez, Elza Rechtman, Ludovic Fillon, et al.

NeuroImage: Clinical 21 (2019) 101610

Contents lists available at ScienceDirect

NeuroImage: Clinical

journal homepage: www.elsevier.com/locate/ynicl

Anatomical and functional abnormalities on MRI in kabuki syndrome

Jennifer Boisgontier[a,*], Jean Marc Tacchella[a], Hervé Lemaître[a,b], Natacha Lehman[c], Ana Saitovitch[a], Vincent Gatinois[c], Guilaine Boursier[c], Elodie Sanchez[c], Elza Rechtman[a], Ludovic Fillon[a], Stanislas Lyonnet[d], Kim-Hanh Le Quang Sang[d], Genevieve Baujat[d], Marlene Rio[d], Odile Boute[e], Laurence Faivre[f], Elise Schaefer[g], Damien Sanlaville[h], Monica Zilbovicius[a], David Grévent[a], David Geneviève[c], Nathalie Boddaert[a]

[a] *Service de radiologie pédiatrique, Hôpital Necker Enfants Malades, INSERM U1000, AP-HP, Université René Descartes, Pres Sorbonne Paris Cité, Institut Imagine, UMR 1163, France*
[b] *Faculté de Médecine, Université Paris Sud, France*
[c] *Département de Génétique Médicale, maladies Rares et Médecine Personnalisée, génétique clinique, CHU Montpellier, Université Montpellier, Centre de référence anomalies du développement SORO, INSERM U1183, Montpellier, France*
[d] *Service de Génétique Médicale, Institut IMAGINE, AP-HP Necker Enfants Malades, France*
[e] *Service de génétique Clinique, Hôpital Jeanne de Flandre, France*
[f] *Service de génétique médicale, Centre de référence anomalies du développement, Fédération Hospitalo-Universitaire Médecine Translationnelle et Anomalies Du Développement (TRANSLAD), Centre Hospitalier Universitaire Dijon, Dijon, France*
[g] *Service de génétique médicale, Institut de Génétique Médicale d'Alsace, Hôpitaux Universitaires de Strasbourg, Strasbourg, France*
[h] *Hospices civils de Lyon, Service de génétique, Centre de Recherche en Neurosciences de Lyon, Inserm U1028, UMR CNRS 5292, GENDEV Team, Université Claude Bernard Lyon 1, Lyon, France*

ARTICLE INFO

Keywords:
Kabuki syndrome
Congenital disorder
Voxel-based morphometry
Arterial spin labeling
Hippocampus
Brodmann area 6 and 9

ABSTRACT

Kabuki syndrome (KS) is a rare congenital disorder (1/32000 births) characterized by distinctive facial features, intellectual disability, short stature, and dermatoglyphic and skeletal abnormalities. In the last decade, mutations in *KMT2D and KDM6A* were identified as a major cause of kabuki syndrome. Although genetic abnormalities have been highlighted in KS, brain abnormalities have been little explored. Here, we have investigated brain abnormalities in 6 patients with KS (4 males; M_{age} = 10.96 years, SD = 2.97 years) with KMT2D mutation in comparison with 26 healthy controls (17 males; M_{age} = 10.31 years, SD = 2.96 years). We have used MRI to explore anatomical and functional brain abnormalities in patients with KS. Anatomical abnormalities in grey matter volume were assessed by cortical and subcortical analyses. Functional abnormalities were assessed by comparing rest cerebral blood flow measured with arterial spin labeling-MRI. When compared to healthy controls, KS patients had anatomical alterations characterized by grey matter decrease localized in the bilateral precentral gyrus and middle frontal gyrus. In addition, KS patients also presented functional alterations characterized by cerebral blood flow decrease in the left precentral gyrus and middle frontal gyrus. Moreover, subcortical analyses revealed significantly decreased grey matter volume in the bilateral hippocampus and dentate gyrus in patients with KS. Our results strongly indicate anatomical and functional brain abnormalities in KS. They suggest a possible neural basis of the cognitive symptoms observed in KS, such as fine motor impairment, and indicate the need to further explore the consequences of such brain abnormalities in this disorder. Finally, our results encourage further imaging-genetics studies investigating the link between genetics, anatomical and functional brain alterations in KS.

Abbreviations: ASL, arterial spin labeling; BA, brodmann area; CBF, cerebral blood flow; DG, dentate gyrus; FWHM, full-width at half-maximum; GLM, general linear model; GM, grey matter; FSIQ, full-scale intelligence quotient; KS, kabuki syndrome; MNI, Montreal Neurological Institute; PRI, perceptive reasoning index; PSI, processing speed index; SMA, supplementary motor area; TE, echo time; TPM, tissue probability map; TR, repetition time; VBM, voxel-based morphometry; VCI, verbal comprehension index; WMI, working memory index

* Corresponding author at: Service de Radiologie Pédiatrique, Hôpital Necker, 149 rue de Sèvres, 75015 Paris, France.
E-mail address: boisgontier.jennifer1414@gmail.com (J. Boisgontier).

https://doi.org/10.1016/j.nicl.2018.11.020
Received 9 April 2018; Received in revised form 16 November 2018; Accepted 18 November 2018
Available online 19 November 2018

1. Introduction

Kabuki syndrome (KS) (OMIM 147920 and OMIM 300867) is a rare genetic disorder (1 in 32,000 births) with five cardinal features: characteristic facial features, dermatoglyphic abnormalities, skeletal malformations, mild to moderate intellectual disability and short stature. Additional features include impaired fine motor skills, susceptibility to infections, visual or auditory impairments, dental abnormalities, and cardiovascular, renal and vertebral malformations (Niikawa et al., 1981). Two major mutations have been described as causing KS: 34% to 76% of KS patients show mutations in KMT2D, a gene that encodes a histone H3 lysine 4 specific methyltransferase needed for H3K4 di- and trimethylation, and < 10% show mutations in KDM6A, a demethylase that removes trimethylation from histone 3 lysine 27 (Bögershausen et al., 2016). These two main genes are involved in transcription and chromatin processes.

Most KS patients have intellectual disability and a heterogeneous intellectual profile. High working memory index (WMI), measuring immediate memory and the ability to concentrate, as well as high verbal comprehension index (VCI), have also been described (Lehman et al., 2017). However, deficits in these functions have also been observed (Mervis et al., 2005; Sanz et al., 2010). In addition, low perceptive reasoning index (PRI), measuring the ability to interpret and organize visual material, as well as low processing speed index (PSI), measuring the ability to process visually perceived material quickly, with concentration and eye-hand coordination, also seem to be part of the KS core neuropsychological profile (Lehman et al., 2017). There is very little literature on the neuropsychological phenotype of KS in humans, which impacts clinical care and reeducation. Interestingly, however, *KMT2D* mutation in a mouse model of KS (*Kmt2d* +/βGeo) revealed hippocampal memory defects, in addition to reduced volume in the granule cell layer of the dentate gyrus (Bjornsson et al., 2014).

Except for a few studies reporting cerebellar and brainstem anomalies (Yano et al., 1997), hippocampal atrophy or perisylvian cortical dysplasia (Takano et al., 2010), we have little information on brain abnormalities in KS. Therefore, the aim of this work was to use MRI to characterize, for the first time, brain abnormalities in KS patients with *KMT2D* mutation compared to healthy controls at different levels. Cortical anatomical abnormalities were primarily explored using whole-brain voxel-based morphometry (VBM). Subcortical hippocampal and dentate gyrus abnormalities were also investigated to extend volumetric results from animal models to humans. Finally, abnormalities in brain functioning at rest were studied using arterial spin labeling (ASL)-MRI to measure rest cerebral blood flow (CBF), without radioactive injection by using water in arterial blood as an endogenous perfusion tracer.

2. Materials and methods

2.1. Participants

We enrolled 9 KS patients (7 males; M_{age} = 10.76 years, range 6 to 15 years) with *KMT2D* mutations (Bögershausen et al., 2016) and 30 healthy controls (20 males; M_{age} = 10.57 years, range 5 to 18 years) with no neurological or psychiatric disorder. All KS patients presenting *KMT2D* mutations (Bögershausen et al., 2016) were recruited from a French research project (PHRC AOM 09-070; ClinicalTrials.gov identifier: NCT01314534). Patients had diagnosis confirmed by an experienced clinical geneticist and presented typical facial gestalt of KS as well as some other features observed in KS (Supplementary table 1). The Wechsler Intelligence Scale for Children, 4th Edition (WISC IV), a full-scale intelligence quotient (FSIQ) clinical instrument, was administered to all participants to evaluate intellectual abilities (Weiss et al., 2006). For each participant, the FSIQ was derived from four index scores: the VCI, perceptive PRI, WMI and PSI.

The experimental protocol was approved by the local ethics committee. After receiving oral and written information about the study, parents of all participants signed an informed consent.

2.2. Experimental design

2.2.1. MRI

3D T1-weighted fast spoiled gradient echo (FSPGR) MRI sequences and ASL-MRI sequences were obtained for all controls. The images were acquired on a 1.5 Tesla (Signa General Electric) MRI scanner at Necker Hospital (Paris, France). 3D T1-weighted FSPGR images were obtained with the following parameters: 240 axial slices, repetition time (TR) = 16.4 ms; echo time (TE) = 7.2 ms; field of view (FOV) = 22 × 22 cm^2; resolution in plane = 0.47*0.47 mm; slice thickness = 1.2 mm. ASL images measuring CBF at rest was performed with pulsed continuous ASL (pseudo continuous). The ASL acquisition parameters were 40 axial slices, TR = 4554 ms; TE = 10.5 ms; FOV = 24 × 24 cm^2; resolution in plane = 1.82*1.82 mm; acquisition matrix = 512 × 8.

2.3. Preprocessing

Seven out of the 39 recruited participants were excluded. Three KS patients were excluded because of dental artefacts (n = 1) and unusable data (n = 2) and 4 healthy controls was excluded because of excessive motion causing faulty segmentation (n = 1) and/or images co-registration (n = 3).

2.3.1. Anatomical study

2.3.1.1. Whole-brain VBM. The images were preprocessed by using Statistical Parametric Mapping 12 (SPM12; Welcome Department of Cognitive Neurology, London, UK, www.fil.ion.ucl.ac.uk/spm). Structural 3D T1-weighted FSPGR images were spatially normalized by using the template from the Montreal Neurological Institute (MNI) and segmented into GM, white matter and cerebrospinal fluid using the CAT12 toolbox and the tissue probability maps in SPM12. The unified segmentation enables spatial normalization, tissue segmentation and bias correction within the same generative model (Ashburner and Friston, 2005). Finally, the normalized, segmented and modulated GM images were smoothed by using a Gaussian kernel of 10-mm full-width at half-maximum (FWHM).

2.3.1.2. Hippocampus and dentate gyrus volumes: Freesurfer method. To specifically investigate the hippocampus, the subcortical regions were segmented using the subcortical segmentation pipeline provided by Freesurfer 6.0 (http://surfer.nmr.mgh.harvard.edu), which allows for an automated volumetric approach (Fischl et al., 2002). Thus, the T1 images were automatically parcellated into 40 labels and we focused on the labels of the left and right hippocampus and corresponding GM volumes. To assess the accuracy of the hippocampal segmentation for each participant, a visual check was performed by two independent operators. Then, we focused on the hippocampus and especially the dentate gyrus (DG) (Patenaude et al., 2011). To extract the volume of the DG from that of the hippocampus bilaterally, we used automated hippocampal subdivisons segmentation with Freesurfer 6.0 (http://surfer.nmr.mgh.harvard.edu).

2.3.2. Functional study

2.3.2.1. Whole-brain rest CBF analysis. For each participant, ASL images were co-registered with native GM images using SPM12. Then, the deformation fields obtained during the spatial normalization of the T1 images were applied to the ASL images to put all images in the same spatial reference. The resulting images were smoothed with a 10-mm FWHM kernel.

2.3.3. Statistical study

2.3.3.1. Whole-brain analysis. Whole-brain voxel-wise comparisons

between patients with KS and healthy controls involved using the general linear model (GLM) framework with SPM12. Analyses were performed on the smoothed, normalized GM and ASL images within a binary GM mask. This mask was built from the mean value of the GM map for all healthy controls with a threshold of 0.2. The significance threshold was set at 0.05 with a Family-Wise-Error correction for multiple comparisons.

2.3.3.2. Hippocampus and DG volume analysis. Group comparisons for bilateral hippocampus and hippocampal subfields volumes involved using the GLM framework with R software (https://www.r-project.org). We considered the group as the main independent factor, and age, laterality, sex and FSIQ score as confounding variables. A Shapiro-Wilk test (Shapiro and Wilk, 1965) was used to assess the normality of data in R software. Data were compared by two-sample *t*-test or chi-square test. $P < .05$ was considered statistically significant.

3. Results

3.1. Participants: demographic and clinical data

The final sample was composed of 6 KS patients (4 males; M_{age} = 10.96 years, SD = 2.97 years) and 26 healthy controls (17 males; M_{age} = 10.31 years, SD = 2.96 years). The groups did not differ by the two-sample t-test for age (t = 0.48; df = 7.47; p = .64) or by chi-square test for laterality (χ^2 = 4.47; df = 1; p = .07) or sex (χ^2 = 0.003; df = 1; p = .95) (Table 1). However, the FSIQ score was significantly lower for KS patients than healthy controls (M_{IQ} = 67.60; SD = 23.42 vs M_{IQ} = 110.85; SD = 11.40) (t = −4.00; df = 4.50; p = .01), (Table 1).

Full clinical, neuropsychological and molecular data for KS patients are summarized in Supplementary Table 1.

3.1.1. Anatomical study

On whole-brain voxel-wise analysis, as compared to healthy controls, KS patients showed significantly decreased GM in bilateral clusters including the precentral gyrus (right: t = 6.67; $z_{(score)}$ = 5.19; $p_{(corr)}$ = 0.008; *MNI coordinates: x = 52 y = 2 z = 45; BA 6* / left: t = 9.30; $z_{(score)}$ = 6.33; $p_{(corr)} = 2.15e^{-7}$*MNI coordinates: x = −58 y = 6 z = 30)* and in the bilateral middle frontal gyrus (right: t = 6.56; $z_{(score)}$ = 5.24; $p_{(corr)}$ = 0.004; *MNI coordinates: x = 42 y = 24 z = 50;* / left: t = 10.12; $z_{(score)}$ = 6.62; $p_{(corr)} = 4.44e^{-6}$; *MNI coordinates: x = −50 y = 28 z = 32*) (Fig. 2 and Fig. 3).

On subcortical analysis, the volumes of the left and right hippocampus were significantly lower in KS patients than in healthy controls [left: (t = 3.93; df = 28; p = .0005) / right: (t = 2.83; df = 28; p = .008)], as was the volumes of the left and right DG [left: (t = 3.11; df = 28; p = .004) / right: (t = 2.73; df = 28; p = .01)] (Table 2). Other hippocampal subfields volume statistics are presented in Supplementary Table 2.

3.1.2. Functional study

Whole-brain voxel-wise analysis revealed a significantly decreased rest CBF in KS patients in clusters including the left precentral gyrus and the left middle prefrontal gyrus (t = 7.02; $z_{(score)}$ = 5.36; $p_{(corr)}$ = 0.001; *MNI coordinates: x = −51 y = 12 z = 30)* (Fig. 1 and Fig. 3).

4. Discussion

To our knowledge, this is the first study to investigate both anatomical and functional brain abnormalities in KS. In light of the KS symptomatology, we provide three main findings. First, at the anatomical level, whole-brain cortical analysis revealed significantly decreased GM in the bilateral precentral gyrus (portion of BA 6) and in the bilateral middle frontal gyrus (portion of BA 9/BA 8) in KS patients when compared to healthy controls. Second, our subcortical analysis, based on previous animal model findings, revealed significantly decreased bilateral hippocampus and DG volumes in KS patients when compared to healthy controls. Finally, at the functional level, rest CBF was significantly decreased in the left precentral gyrus (portion of BA 6) and the left middle frontal gyrus (portion of BA 9/BA 8) in KS patients.

Abnormalities localized in BA 6 and BA 9 are relevant in light of the cognitive symptomatology observed in KS patients (Matsumoto and Niikawa, 2003). In the literature, BA 6 is situated in the frontal cortex anterior to the primary motor cortex (BA 4) and represents a portion of the precentral gyrus. BA 6, including the premotor cortex and the supplementary motor area, is considered critical for the sensory guidance of movement and movement initiation. Pertinently, BA 6 extends onto the caudal portion of the dorsolateral prefrontal cortex, corresponding to BA 9, another abnormal region we found in KS patients. Moreover, the supplementary motor area (which is part of BA 6) receives projections from BA 9, which plays an important role in motor organization, planning and regulation (Nakayama and Hoshi, 2017). Damage in BA 6 and BA 9 may result in the motor apraxia or dyspraxia reported in neurodegenerative disorders or frontal syndrome (Gross and Grossman, 2008). Thus, abnormalities in both BA 6 and BA 9 in KS patients may explain in part the motor function impairments they present.

Recent descriptions have highlighted the attenuation of the distal interphalangeal crease of the third and fourth finger as a particular clinical sign in KS patients (Michot et al., 2013). This attenuation could be associated with the lack of digits motor activity, a characteristic developed in KS patients, which could result from abnormalities in regions involved in motor processing such as BA 6 and BA 9, described in our results. However, even though the presence of very stable fine-grain somatotopy of the digits was recently demonstrated in the human primary somatosensory cortex, further functional investigations are needed to confirm this hypothesis (Kolasinski et al., 2016).

We also found a significant decrease in volume of the bilateral hippocampus in KS patients when compared to healthy controls. These structural abnormalities of the hippocampus agree with previous animal studies. Indeed, using a mouse model of KS (Kmt2d +/βGeo), Bjornsson et al. reported hippocampal memory deficits evaluated by the Morris Water Maze (Bjornsson et al., 2014). The hippocampus, a structure localized in the temporal lobe, plays a crucial role in the consolidation of episodic memory, learning and spatial coding (Jonas and Lisman, 2014). Considering its established functional role in

Table 1
Clinical and demographic data for patients with KS and healthy controls.

	Kabuki syndrome participants (n = 6)	Healthy participants (n = 26)	Statistics	*df*	*p*
Age, mean [SD]	10.96 [2.97]	10.31 [2.96]	t = 0.48	7.47	0.64
Sex (M; F)	4; 2	17; 9	χ^2 = 0.003	1	0.95
Laterality (RH; LH)	5; 1	26; 0	χ^2 = 4.47	1	0.07
FSIQ, mean [SD]	67.60 [23.42]	110.85 [11.40]	t = −4.00	4.50	0.01*

Abbreviations: SD: Standard Deviation; M: male; F: female; LH: left-handed; RH: right-handed; FSIQ: full-scale intellectual quotient.
* p < .05.

Table 2
Volume of hippocampus and dentate gyrus in patients with KS and healthy controls.

Volume of:	KS participants (n = 6)	Healthy controls (n = 26)	Statistics	*df*	*p*
Left hippocampus (in mm^3), mean [SD]	3283.06 [510.45]	3814.43 [336.94]	$t = 3.93$	28	0.0005*
Right hippocampus (in mm^3), mean [SD]	3427.31 [624.17]	3855.47 [373.06]	$t = 2.83$	28	0.008*
Left dentate gyrus (in mm^3), mean [SD]	230.65 [38.24]	268.53 [29.41]	$t = 3.11$	28	0.004*
Right dentate gyrus (in mm^3), mean [SD]	247.47 [38.69]	278.83 [32.90]	$t = 2.73$	28	0.01*

Abbreviations: SD: Standard Deviation; df: degrees of freedom.
* $p < .05$

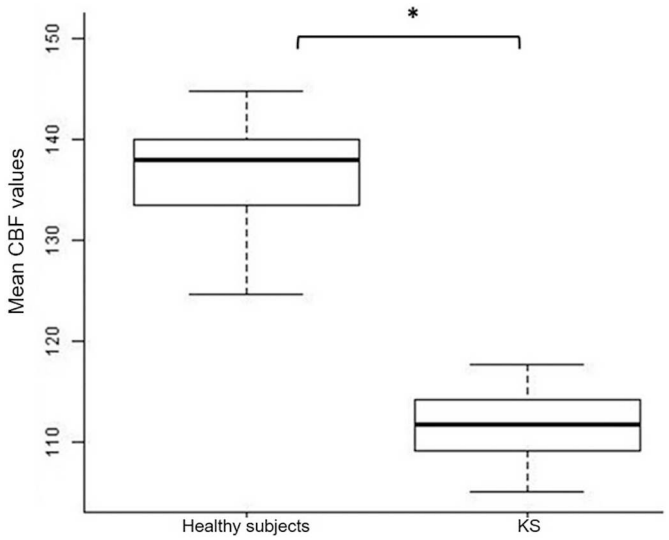

Fig. 1. Box plot comparisons of rest CBF values between groups. Between group comparison of mean rest cerebral blood flow values in the left precentral gyrus and in the middle frontal gyrus.
Abbreviations: KS: kabuki syndrome; CBF: cerebral blood flow; ASL: arterial spin labelling.
*$p < .05$.

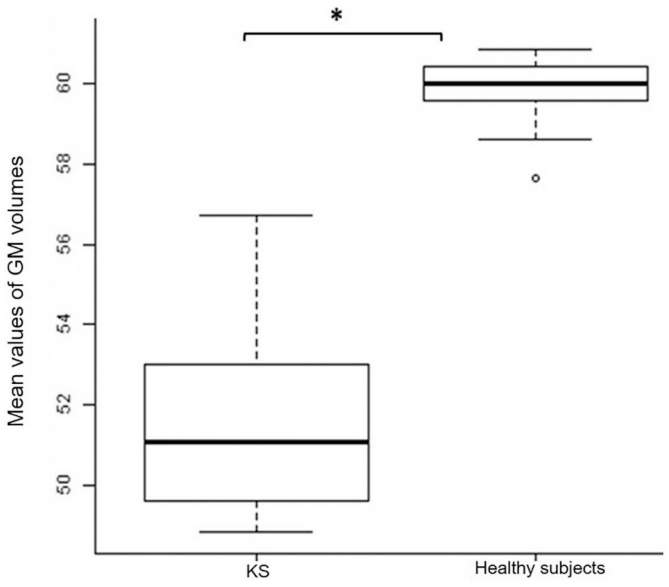

Fig. 2. Box plot comparisons of GM volumes between groups. Between group comparison of mean GM volumes within significant clusters from VBM analyses in the bilateral precentral gyrus and in the middle frontal gyrus.
Abbreviations: KS: kabuki syndrome; CBF: cerebral blood flow; ASL: arterial spin labelling.
*$p < .05$.

memory function, abnormalities in the hippocampus could affect neuropsychological processes in KS. Recent results of neuropsychological studies in KS (Lehman et al., 2017) have describe high WMI scores in KS patients. However, it's worth noticing that the WMI, largely used to evaluate memory in KS patients, evaluates only working memory and not all other aspects of memory. Our results suggest that specific memory tests may be needed to further understand the link between episodic memory, working memory and hippocampal substrate.

Although several subdivisions of the hippocampus showed lower volumes in KS patients compared to healthy subjects, our significant result in the bilateral DG is of particular interest in regard to previous results in animal studies. Indeed, Kmt2d +/βGeo mice showed reduced volume of the DG granule-cell layer, which was associated with hippocampal memory defect (Bjornsson et al., 2014). The DG, an input to the hippocampus, is one of the brain regions able to continuously generate neurons, commonly called neurogenesis (Brus et al., 2013). Pertinently, the main mutation reported in KS is a protein highly expressed in the DG, which could underlie the abnormalities described (Bjornsson et al., 2014). These hippocampal abnormalities may be associated with memory impairments observed in the mouse model of KS. At the functional level, the main role of the DG is supposedly to mediate mnemonic processing of spatially based events (Kesner, 2013). In this regard, 11 adolescents with KS showed a clear weakness in visuospatial construction, which suggests visuospatial deficits in KS patients (Mervis et al., 2005). More recently, Lehman et al. found weaknesses in PRI, which was related to visuospatial abilities, in the intellectual profile of 31 children with KS (Lehman et al., 2017). These results might be linked to spatial memory deficits, but deeper evaluation of spatial memory is needed to clarify this link. In view of the structural organization of the DG, namely that it receives visual and auditory inputs from the perirhinal and lateral entorhinal cortex (Amaral et al., 2007), the anatomical abnormalities of the DG in KS patients we report may be associated with visual or auditory impairments observed in KS. In this regard, Lehman et al. demonstrated visual anomalies in KS associated with a 10-point reduction in FSIQ as compared to KS patients with no visual problems. These data indicate that visual as well as visuospatial anomalies are also key features in the intellectual disability in KS.

Previous results from animal models suggested that *KMT2D* has a functional role in the brain. Indeed, Laarhoven et al. reported a reduced size of the brain and abnormal embryonic development of the ventricles and midbrain in zebrafish simulating haploid sufficiency of the *KMT2D* mutation (Van Laarhoven et al., 2015), which suggests a crucial functional role of *KMT2D* in embryonic development of the brain. Our results suggest a functional role of *KMT2D* also in the human brain.

Because of the small prevalence of KS (1/32000 births) (Geneviève et al., 2004), our study is based on a fairly small sample, which could in general imply overestimation of the effect and low statistical power. However, all KS patients in this study shared mutations in the same gene, *KMT2D*, which preserves the homogeneity of our sample and reduces the potential variability bias of our results.

5. Conclusion

Here we provide evidence of structural and functional brain

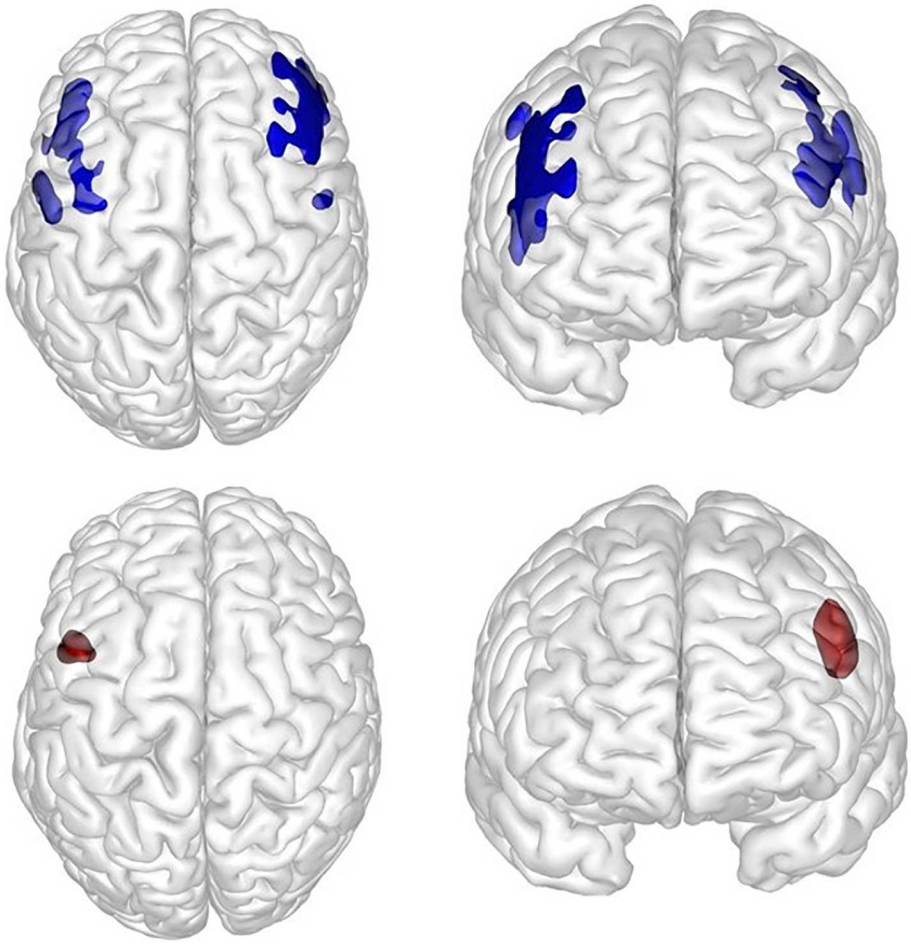

Fig. 3. Axial and sagittal 3D views of the significant clusters from VBM and ASL analyses. Axial and sagittal 3D views of the clusters including the bilateral precentral gyrus and the bilateral middle frontal gyrus (in blue) obtained from VBM analyses and the left precentral gyrus and the middle frontal gyrus (in red) from the ASL-MRI rest cerebral blood flow analysis.

alterations in patients with KS. We demonstrate significant GM and rest CBF abnormalities localized in the precentral gyrus (portion of BA 6) and middle frontal gyrus (portion of BA 9 / BA 8) in KS patients, which could support a brain substrate of the fine motor skills deficits in these patients. In addition, the bilateral decrease in volume of the hippocampus and DG we observed may play a crucial role in the cognitive symptomatology of KS. To warrant the behavioral relevance of our findings, specific neuropsychological assessments of memory processes are needed. Moreover, further complementary exploration of white-matter integrity between BA 6 and BA 9 in the same sample would be an important perspective to examine structural connectivity in KS. Finally, our results strongly indicate the relevance of brain imaging investigations in KS and open up perspectives for broader investigations in innovative research fields, such as imaging-genetics, to elucidate the pathophysiology of this syndrome, still poorly known.

Supplementary data to this article can be found online at https://doi.org/10.1016/j.nicl.2018.11.020.

Acknowledgments

The authors thank the participating staff of the centers and the participants of this study. We are grateful to the families for their help and participation. We thank the French Kabuki association http://www.syndromekabuki.fr for their participation.

Funding sources

Part of this work was supported by the French Ministry of Health (Programme Hospitalier de Recherche Clinique national AOM 07-090), Fondation Maladies Rares, and the French Kabuki Associationhttp://www.syndromekabuki.fr/. We thank the French Kabuki Association for their help in this study.

Conflict of interest disclosures

The authors have no financial conflicts of interest to disclose.

References

Amaral, D.G., Scharfman, H.E., Lavenex, P., 2007. The dentate gyrus: fundamental neuroanatomical organization (dentate gyrus for dummies). Prog. Brain Res. 163, 3–22.
Ashburner, J., Friston, K.J., 2005. Unified segmentation. NeuroImage 26, 839–851.
Bjornsson, H.T., Benjamin, J.S., Zhang, L., Weissman, J., Gerber, E.E., Chen, Y.-C., et al., 2014. Histone deacetylase inhibition rescues structural and functional brain deficits in a mouse model of Kabuki syndrome. Sci. Transl. Med. 6, 256ra135.
Bögershausen, N., Gatinois, V., Riehmer, V., Kayserili, H., Becker, J., Thoenes, M., et al., 2016. Mutation update for kabuki syndrome genes KMT2D and KDM6A and further delineation of X-linked kabuki syndrome subtype 2. Hum. Mutat. 37, 847–864.
Brus, M., Keller, M., Lévy, F., 2013. Temporal features of adult neurogenesis: differences and similarities across mammalian species. Front. Neurosci. 7, 135.
Fischl, B., Salat, D.H., Busa, E., Albert, M., Dieterich, M., Haselgrove, C., et al., 2002. Whole brain segmentation: automated labeling of neuroanatomical structures in the human brain. Neuron 33, 341–355.
Geneviève, D., Amiel, J., Viot, G., Le Merrer, M., Sanlaville, D., Urtizberea, A., et al., 2004. Atypical findings in Kabuki syndrome: report of 8 patients in a series of 20 and review of the literature. Am. J. Med. Genet. A 129A, 64–68.

Gross, R.G., Grossman, M., 2008. Update on apraxia. Curr. Neurol. Neurosci. Rep. 8, 490.
Jonas, P., Lisman, J., 2014. Structure, function, and plasticity of hippocampal dentate gyrus microcircuits. Front. Neural Circuits 8.
Kesner, R.P., 2013. An analysis of the dentate gyrus function. Behav. Brain Res. 254, 1–7.
Kolasinski, J., Makin, T.R., Jbabdi, S., Clare, S., Stagg, C.J., Johansen-Berg, H., 2016. Investigating the stability of fine-grain digit somatotopy in individual human participants. J. Neurosci. 36, 1113–1127.
Lehman, N., Mazery, A.C., Visier, A., Baumann, C., Lachesnais, D., Capri, Y., et al., 2017 Sep. Molecular, clinical and neuropsychological study in 31 patients with Kabuki syndrome and KMT2D mutations. Clin. Genet. 92 (3), 298–305. https://doi.org/10.1111/cge.13010. Epub 2017 May 18.
Matsumoto, N., Niikawa, N., 2003. Kabuki make-up syndrome: A review. Am. J. Med. Genet. C Semin. Med. Genet. 117C, 57–65.
Mervis, C.B., Becerra, A.M., Rowe, M.L., Hersh, J.H., Morris, C.A., 2005. Intellectual abilities and adaptive behavior of children and adolescents with Kabuki syndrome: a preliminary study. Am. J. Med. Genet. A 132A, 248–255.
Michot, C., Corsini, C., Sanlaville, D., Baumann, C., Toutain, A., Philip, N., et al., 2013. Finger creases lend a hand in Kabuki syndrome. Eur. J. Med. Genet. 56, 556–560.
Nakayama, Y., Hoshi, E., 2017. Cortical areas for controlling voluntary movements. Brain Nerve Shinkei Kenkyu No Shinpo 69, 327–337.
Niikawa, N., Matsuura, N., Fukushima, Y., Ohsawa, T., Kajii, T., 1981. Kabuki make-up syndrome: a syndrome of mental retardation, unusual facies, large and protruding ears, and postnatal growth deficiency. J. Pediatr. 99, 565–569.
Patenaude, B., Smith, S.M., Kennedy, D.N., Jenkinson, M., 2011. A Bayesian model of shape and appearance for subcortical brain segmentation. NeuroImage 56, 907–922.
Sanz, J.H., Lipkin, P., Rosenbaum, K., Mahone, E.M., 2010. Developmental profile and trajectory of neuropsychological skills in a child with Kabuki syndrome: implications for assessment of syndromes associated with intellectual disability. Clin. Neuropsychol. 24, 1181–1192.
Shapiro, S.S., Wilk, M.B., 1965. An analysis of variance test for normality (complete samples). Biometrika 52, 591–611.
Takano, T., Matsuwake, K., Yoshioka, S., Takeuchi, Y., 2010. Congenital polymicrogyria including the perisylvian region in early childhood. Congenit. Anom. 50, 64–67.
Van Laarhoven, P.M., Neitzel, L.R., Quintana, A.M., Geiger, E.A., Zackai, E.H., Clouthier, D.E., et al., 2015. Kabuki syndrome genes KMT2D and KDM6A: functional analyses demonstrate critical roles in craniofacial, heart and brain development. Hum. Mol. Genet. 24, 4443–4453.
Weiss, L.G., Saklofske, D.H., Prifitera, A., Holdnack, J.A., 2006. WISC-IV Advanced Clinical Interpretation. Elsevier.
Yano, S., Matsuishi, T., Yoshino, M., Kato, H., Kojima, K., 1997. Cerebellar and brainstem 'atrophy' in a patient with Kabuki make-up syndrome. Am. J. Med. Genet. 71, 486–487.